

This is the accepted manuscript made available via CHORUS. The article has been published as:

Nuclear Matrix Elements for Tests of Local Lorentz Invariance Violation

B. A. Brown, G. F. Bertsch, L. M. Robledo, M. V. Romalis, and V. Zelevinsky

Phys. Rev. Lett. **119**, 192504 — Published 8 November 2017

DOI: [10.1103/PhysRevLett.119.192504](https://doi.org/10.1103/PhysRevLett.119.192504)

Nuclear Matrix Elements for Tests of Local Lorentz Invariance Violation

B. A. Brown¹, G. F. Bertsch², L. M. Robledo³, M. V. Romalis⁴ and V. Zelevinsky¹

¹ *Department of Physics and Astronomy and National Superconducting Cyclotron Laboratory, Michigan State University, East Lansing, Michigan 48824-1321, USA*

² *Institute for Nuclear Theory and Department of Physics, Box 351560, University of Washington, Seattle, Washington 98195, USA*

³ *Departamento de Fisica Teorica, Modulo 15, Universidad Autonoma de Madrid, E-28049 Madrid, Spain and*

⁴ *Department of Physics, Princeton University, Princeton, New Jersey 08544, USA*

The nuclear matrix elements for the momentum quadrupole operator are important for the interpretation of precision atomic physics experiments that search for violations of local Lorentz and CPT symmetry and for new spin-dependent forces. We use the configuration-interaction nuclear shell model and self-consistent mean field theory to calculate these matrix elements in ²¹Ne, ²³Na, ¹³¹Xe, ¹⁷³Yb and ²⁰¹Hg. These are the first microscopic calculations of the nuclear matrix elements for the momentum quadrupole tensor that go beyond the single-particle estimate. We show that they are strongly suppressed by the many-body correlations, in contrast to the well known enhancement of the spatial quadrupole nuclear matrix elements.

PACS numbers: 21.60.Cs, 21.60.Ev, 04.80.Cc

Several types of precision low energy tests of the Standard Model use nuclear-spin-polarized atoms to achieve very high sensitivity by relying on long nuclear spin coherence times that are possible with atoms in ¹S₀ ground state, such as ³He, ²¹Ne, ¹²⁹Xe, ¹³¹Xe, ¹⁷³Yb, ¹⁹⁹Hg and ²⁰¹Hg. Such tests include searches for violation of local Lorentz and CPT symmetry [1], [2], [3], [4], and for new spin-dependent forces mediated by light particles, such as an axion [5], [6], [7], [8], [9], [10].

The interpretation and comparison of these experiments requires knowledge of nuclear matrix elements responsible for new interactions beyond the Standard Model. A number of simple models have been used to estimate the relevant nuclear matrix elements [11], [12], [13], [14], [15], [16]. but few detailed nuclear structure calculations have been performed so far for this purpose. This can be contrasted with a large number of nuclear structure calculations performed to estimate the scattering cross-sections for dark matter particles [17], [18], [19] and rates for neutrinoless double-beta decay [20].

The nuclear matrix elements relevant in searches for local Lorentz invariance violation (LLIV) within the Standard Model Extension (SME) are derived in [11]. Here we focus on matrix elements that generate couplings to CPT-odd b_μ and CPT-even $c_{\mu\nu}$ terms in the SME Lagrangian for fermions:

$$\mathcal{L} = \frac{1}{2} i \bar{\psi} (\gamma_\nu + c_{\mu\nu} \gamma^\mu) \overleftrightarrow{\partial}^\nu \psi - \bar{\psi} (m + b_\mu \gamma_5 \gamma^\mu) \psi. \quad (1)$$

For non-relativistic nucleon motion they generate an energy shift

$$\mathcal{H} = -2b_j S_j - (c_{jk} + c_{00} \delta_{jk}/2) p_j p_k / m, \quad (2)$$

where S_j is the spin operator, p_j is the momentum operator, and m is the mass of the fermion. Traditionally, LLIV effects and spin-dependent forces have been analyzed separately at the level of neutrons and protons under the assumption that they are independent. This provides a way to roughly classify the experiments without making assumptions about a microscopic theory that would likely generate comparable effects in neutrons and protons. For particles that are on average at rest, only the spherical rank-2 components of the tensor $p_i p_j$ give a finite energy shift. Using Wigner-Eckart theorem, they can be expressed in terms of the matrix elements of the momentum quadrupole tensor operator $\hat{M} = 2p_z^2 - p_x^2 - p_y^2$,

$$M = \langle I, I | \hat{M} | I, I \rangle = \langle I, I | 2p_z^2 - p_x^2 - p_y^2 | I, I \rangle, \quad (3)$$

for a nucleus with spin I and its projection $I_z = I$. In the nucleus there are two components for this, proton, M_p , and neutron, M_n . The best current limits on LLIV effects currently come from the quadrupole momentum matrix element in the nucleus ²¹Ne [4]. The calculations for ²¹Ne [4] were based on a simple single-particle estimate for the odd valence neutron. Flambaum et al. [14], [16] have presented a model where momentum quadrupole moment (M) is related to the experimental spatial quadrupole moment (Q)

$$Q = \langle I, I | \hat{Q} | I, I \rangle = \langle I, I | 2z^2 - x^2 - y^2 | I, I \rangle, \quad (4)$$

with two components Q_p and Q_n .

In addition to ²¹Ne (odd nucleon), in this letter we consider four other nuclei that all have $I \geq 3/2$ that is

required for the tensor matrix elements to be nonzero. Three heavy nuclei ^{133}Cs (odd proton), ^{173}Yb (odd neutron), and ^{201}Hg (odd neutron) are used widely for atomic NMR studies. ^{133}Cs can be used in an alkali-metal co-magnetometer, using techniques similar to [21]. ^{173}Yb can be used using an optical dipole trap [1]. LLIV for ^{201}Hg was studied in [22]. For consistency we also consider the odd-proton sd shell nucleus ^{23}Na . We present self-consistent mean-field model (SCMF) calculations for all of these nuclei that are consistent with the experimental Q for protons. For heavy nuclei the momentum matrix elements M are close to zero within the theoretical uncertainty. We give a simple explanation for this result. These results are inconsistent with previous calculations [14], [16]. For ^{21}Ne and ^{23}Na we compare the SCMF results to those from the configuration interaction (CI) shell model. Within the CI model it is essential to include core polarization that reduces the momentum matrix elements compared to those obtained in the sd shell valence space. The consistency of the SCMF and CI results for ^{21}Ne and ^{23}Na suggest small but robust non-zero values for the tensor momentum matrix elements.

The SCMF model has proved to be quite reliable for calculating matrix elements of one-body operators such as the Q in deformed nuclei [24]. Here we use the Hartree-Fock-Bogoliubov method [25], [26], with the Gogny D1S interaction [27]. The odd-particle orbital is blocked and time-odd fields are taken into account in the self-consistent process. Axial symmetry is preserved so that the different mean field configurations can be labeled with the K quantum number of deformed nuclei. Reflection symmetry is allowed to be broken, but in the isotopes treated here parity remains a good quantum number. SCMF results for ^{21}Ne , ^{133}Cs , ^{173}Yb and ^{201}Hg are shown in Figs. 1 and 2 as a function of the deformation parameter β_2 . For ^{133}Cs and ^{201}Hg the energy has a broad minimum around $\beta_2=0$, whereas ^{21}Ne and ^{173}Yb have a large prolate deformation.

The experimental Q values as shown in these figures lie near the SCMF energy minimum. The M cross zero near where the SCMF energy has a minimum. These results imply $|M_p| < 10$ and $|M_n| < 10$ (in units of m MeV). A more precise limit or a non-zero value might be obtainable if the calculations were extended beyond mean field to include fluctuations around the energy minima, for example by generator coordinate method (GCM). For ^{133}Cs , ^{173}Yb and ^{201}Hg , these limits are a factor of five smaller than the values obtained Flambaum et al. [14], [16], because they do not take into account the total energy minimization.

The reason for this result can be seen easily with a very simple density-functional model which generalizes the harmonic oscillator model of Bohr and Mottelson [28].

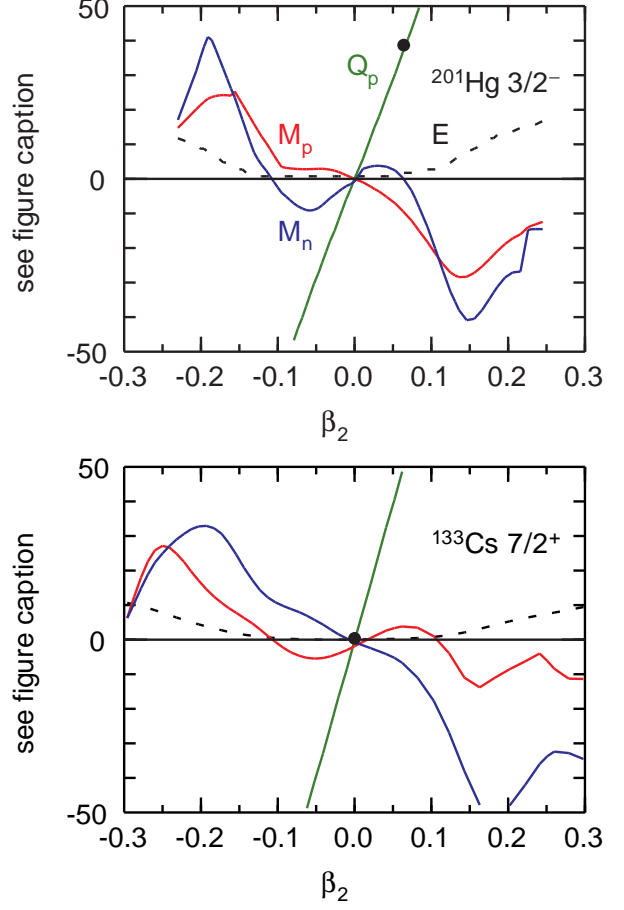


FIG. 1: Results of the SCMF calculations for ^{133}Cs and ^{201}Hg . Four curves are shown as a function of the constrained β_2 value. The dashed line labeled E is the SCMF energy in units of MeV relative to its minimum. The green line labeled Q_p is the charge quadrupole moment in units of $e \text{ fm}^2$. The blue line labeled M_n is the neutron momentum quadrupole moment in units of m MeV, where m is the nucleon mass. The blue line labeled M_p is the proton momentum quadrupole moment in units of m MeV. The experimental charge quadrupole moment [23] is shown by the black circle on the green line.

We take the energy functional as

$$E = \langle \Psi | \frac{p^2}{2m} | \Psi \rangle + \int d^3r \mathcal{V}[\rho(r)], \quad (5)$$

where \mathcal{V} is an interaction-energy functional depending only on the local density $\rho(r) = \langle \Psi | a_r^\dagger a_r | \Psi \rangle$. Consider the change in energy when the wave function is changed by the scaling transformation for the i nucleons $\Psi'(r_i) = \Psi(r'_i)$ where $r' = (x', y', z') = (x e^{-\varepsilon/2}, y e^{-\varepsilon/2}, z e^{\varepsilon})$. The interaction energy remains the same with the new wave function because the Jacobian for the transformation of variables is unity, ie. $d^3r = d^3r'$. The kinetic

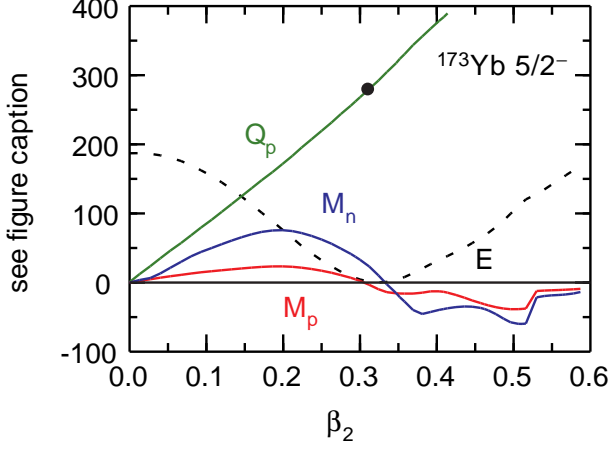


FIG. 2: Results of the SCMF calculations for ^{173}Yb . The labels and units are the same as Fig. 1, except that E has been multiplied by 10.

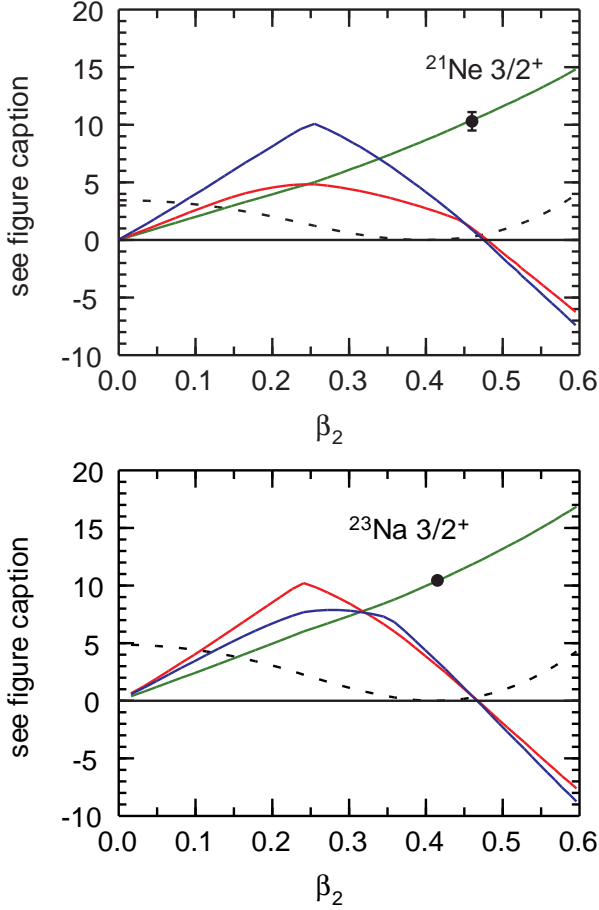


FIG. 3: Results of the SCMF calculations for ^{21}Ne and ^{23}Na . The labels and units are the same as Fig. 1.

term does change, depending on ε as

$$\frac{1}{2m}\langle p^2 \rangle^\varepsilon = \frac{1}{2m} (\langle p_x^2 \rangle e^\varepsilon + \langle p_y^2 \rangle e^\varepsilon + \langle p_z^2 \rangle e^{-2\varepsilon}). \quad (6)$$

The energy is minimum in the ground state implying $d\langle T \rangle^\varepsilon / d\varepsilon = 0$. Carrying out the algebra, one finds that the derivative vanishes only if $M = 2\langle p_z^2 \rangle - \langle p_x^2 \rangle - \langle p_y^2 \rangle = 0$. As discussed in [28], the equilibrium condition is the isotropy of the velocity distribution; it is also related to the Bohr-van Leeuwen theorem of absence of magnetization in the equilibrated classical gas of charged particles. This result applies to the isoscalar combination of the M values, $M_p + M_n$. It is possible that there is still some non-zero isovector component to M (proportional to $M_p - M_n$). Also the momentum-dependent part of the interaction could give some non-zero isoscalar part. There is an implicit momentum dependence associated with the exchange operators built into the D1S. Also, the spin-orbit term involves the momentum explicitly. But the D1S interaction is dominated by the central terms.

In [4] the matrix element for ^{21}Ne was obtained from the simple assumption that it is described by a neutron in the $0d_{3/2}$ orbital outside of a ^{20}Ne core. The result from this model is given in Table I. This simple model does not reproduce the experimental value for Q_p . ^{21}Ne is better described in the full $0d_{5/2}, 1s_{1/2}, 0d_{3/2}$ (sd) shell-model basis with USDB Hamiltonian that has been globally validated on properties of nuclei in that mass region [29]. For ^{21}Ne the spin matrix elements assuming the simple $0d_{3/2}$ model are $\langle S_{zp} \rangle = 0$ and $\langle S_{zn} \rangle = -0.3$ and the magnetic moment is $\mu = 1.148$. The full sd CI results are $\langle S_{zp} \rangle = 0.022$ and $\langle S_{zn} \rangle = 0.292$ and $\mu = -0.720$. The latter is in reasonable agreement with the experimental value of $\mu_{exp} = -0.662$.

The CI results for the quadrupole matrix elements are given in Table I. The calculated Q_p is about a factor of two smaller than experiment. It is well known that the quadrupole observables require an effective charge [30]. This comes from core polarization that is related to the admixture of the giant quadrupole resonance at an oscillator energy of $2\hbar\omega$. Thus the quadrupole moments are calculated as

$$Q_p = Q_p^{sd}(1 + \delta_{pp}) + Q_n^{sd}\delta_{np},$$

and

$$Q_n = Q_n^{sd}(1 + \delta_{nn}) + Q_p^{sd}\delta_{pn}. \quad (7)$$

where δ_{vc} are the corrections due to the polarization of the core nucleons (c) by the valence nucleons (v). For $N \sim Z$ one can use $\delta_{pp} = \delta_{nn} = \delta_p$ and $\delta_{pn} = \delta_{np} = \delta_n$. Values of $\delta_p = 0.36$ and $\delta_n = 0.45$ are the effective charge parameters appropriate for sd -shell E2 observables [30]. The results with these effective charges are in Table I labeled CI + CP. With effective charges the Q_p is enhanced and agrees with experiment. We can also note that the

TABLE I: Quadrupole matrix elements for ^{21}Ne , $I^\pi=3/2^+$. CP is the core-polarization correction. The experimental value is from [23].

	Q_p fm ²	Q_n fm ²	M_p m MeV	M_n m MeV
experiment	10.3(8)			
$\nu 0d_{3/2}$	0	-4.5	0	-18.2
CI	5.4	6.4	21.9	25.9
CI + CP	10.2	11.0	2.7	7.0
SCMF	8.6	9.7	2.8	4.2

consideration of small deformations in [16] is not reliable as quantum fluctuations become very large.

The same polarization physics applies for the momentum anisotropy operator, but with the opposite sign of the effective charge. The expression is the same as Eqs. (7) but with Q replaced by M and a change of sign for all of the δ . The sign may be seen from the perturbative formula for the polarization contribution to the moment of an operator \mathcal{O} ,

$$\delta\mathcal{O} = \sum_{p,h} \langle p | V | h \rangle \frac{1}{E_p - E_h} \langle p | \mathcal{O} | h \rangle, \quad (8)$$

where p, h are particle and hole orbitals. For harmonic oscillator orbitals p and h are two major shells apart ($\Delta N = 2$ where $N = 2n + \ell$), and the matrix elements of the operators \hat{Q} and \hat{M} are related by

$$\langle p | \hat{Q} | h \rangle = -\frac{1}{m^2\omega_0^2} \langle p | \hat{M} | h \rangle. \quad (9)$$

where ω_0 is the oscillator frequency. Applying the above effective charges with the opposite sign, we obtain the M given in Table I. The M are strongly reduced by core-polarization. The SCMF results at the energy minimum of Fig. 2 are given in the last line of Table I. The CI and SCMF results are fairly consistent. Given this consistency, we suggest that the M matrix elements for ^{21}Ne are small but not zero; $M_p = 3(1)$ and $M_n = 5(2)$ m MeV.

In summary, we have presented new calculations for the momentum matrix elements relevant for low-energy tests of local Lorentz invariance violation involving polarized nuclear spins. With our self-consistent mean-field (SCMF) calculations we showed that momentum quadrupoles are small, and explain this using a variational principle for the energy with momentum-independent interactions. Previous calculations by Flambaum [14], [16] make a connection between the experimental spatial quadrupole moment and the momentum quadrupole moments. In contrast, we find that these two kinds of moments are not connected, the spatial matrix element is strongly enhanced in deformed nucleus, but

TABLE II: Quadrupole matrix elements for ^{23}Na , $I^\pi=3/2^+$. CP is the core-polarization correction. The experimental value is from [23].

	Q_p fm ²	Q_n fm ²	M_p m MeV	M_n m MeV
experiment	10.45(10)			
CI	5.8	6.3	23.7	25.2
CI + CP	10.7	11.2	3.6	5.9
SCMF	10.3	11.3	3.2	3.6

the momentum matrix element is small and close to zero in the nuclei studied here.

For the heavy nuclei the best we can do with the SCMF model is to place an upper limit on the quadrupole momentum matrix element M of about 10 m MeV. But the M values are not zero, and until better calculations can be done, we would suggest a nominal value of one m MeV be used to interpret LLIV experiments for heavy nuclei. Even though this is much smaller than Flambaum's estimates [14], [16], it still provides useful constraints on the non-standard model parameters from LLIV experiments.

The GCM often used in nuclear physics to deal with quantum correlations beyond the mean field require overlaps of operators between Hartree-Fock-Bogoliubov wave functions. The explicit form of those overlaps do depend on the quantum numbers of the system, and time-odd effects have to be considered in odd-A nuclei. As a consequence, just a very small fraction of the GCM calculations so far have addressed odd systems (see Ref. [31] for a recent example, that includes symmetry restorations). Recent advances in the techniques required [32] suggest that GCM computer codes for odd-A systems will become available soon and will be as popular as the ones for even-even systems. As the computational cost of the GCM scales moderately with mass number A , the new developments will allow calculations in both light and heavy nuclear systems.

For ^{21}Ne and ^{23}Na we use both the SCMF and configuration interaction models. The consistency of these models provides some confidence in a non-zero M value that involves both protons and neutrons. Previously, a simple model based on a valence neutron was used to put limit on the LLIV non-standard model parameters for the neutron [4]. Our result implies that this limit should be applied to a combination of proton and neutron that is approximately the isoscalar combination of the two. The M moments should be calculated in ab-initio approaches to light nuclei [33], [34], [35], to check the results obtained in the more phenomenological models used here.

Acknowledgements: We would like to acknowledge discussions with Michael Hohensee and Victor Flambaum. BAB and VZ were supported in part by NSF grant PHY-

1404442 and by the grant from the Binational Science Foundation US-Israel. GB was supported in part by U.S. Dept. of Energy grant No. DE-FG02-00ER41132. LMR was supported in part by the Spanish grants Nos. FPA2015-65929 MINECO and FIS2015-63770 MINECO, and by the Consolider Ingenio 2010 program MULTIDARK CSD2009-00064. MVR was supported in part by NSF grant PLR-1142032

-
- [1] M. Bishof et al., Phys. Rev. C **94**, 025501 (2016).
 - [2] F. Canee, D. Bear, D. F. Phillips, M. S. Rosen, C. L. Smallwood, R. E. Stoner, R. L. Walsworth, and V. A. Kostelecký, Phys. Rev. Lett. **93**, 230801 (2004).
 - [3] J. M. Brown, S. J. Smullin, T. W. Kornack, and M. V. Romalis, Phys. Rev. Lett. **105**, 151604, (2010).
 - [4] M. Smicklas, J. M. Brown, L. W. Cheuk, S. J. Smullin, and M. V. Romalis, Phys. Rev. Lett. **107**, 171604 (2011).
 - [5] B. J. Venema, P. K. Majumder, S. K. Lamoreaux, B. R. Heckel, and E. N. Fortson, Phys. Rev. Lett. **68**, 135, (1992).
 - [6] A. N. Youdin, D. Krause, Jr., K. Jagannathan, L. R. Hunter, and S. K. Lamoreaux, Phys. Rev. Lett. **77**, 2170 (1996).
 - [7] G. Vasilakis, J. M. Brown, T. W. Kornack, and M. V. Romalis, Phys. Rev. Lett. **103**, 261801 (2009).
 - [8] M. Bulatowicz, R. Griffith, M. Larsen, J. Mirijanian, C. B. Fu, E. Smith, W. M. Snow, H. Yan, and T. G. Walker, Phys. Rev. Lett. **111**, 102001 (2013).
 - [9] K. Tullney *et. al*, Phys. Rev. Lett. **111**, 100801 (2013).
 - [10] L. Hunter, J. Gordon, S. Peck, D. Ang, J. Lin, Science, **339**, 928 (2013).
 - [11] R. Bluhm, V. A. Kostelecký, C. D. Lane, and N. Russell, Phys. Rev. Lett. **88**, 090801 (2002).
 - [12] Y. V. Stadnik and V. V. Flambaum, Eur. Phys. J. C **75**, 110 (2015); J. C. Berengut, V. V. Flambaum, and E. M. Kava, Phys. Rev. A **84**, 042510 (2011); V. V. Flambaum and A. F. Tedesco, Phys. Rev. C **73**, 055501 (2006);
 - [13] D. F. Jackson-Kimball, New J. Phys. **17** 073008 (2015).
 - [14] V. V. Flambaum, Phys. Rev. Lett. **117**, 072501 (2016).
 - [15] V. V. Flambaum and M. V. Romalis, Phys. Rev. Lett. **118**, 142501 (2017).
 - [16] B. G. C. Lackenby and V. V. Flambaum, arXiv:1705.02642v1.
 - [17] V. A. Bednyakov and F. Simkovic, Phys. Part. Nucl. **36**, 131 (2005)
 - [18] P. Klos, J. Menendez, D. Gazit, and A. Schwenk, Phys. Rev. D **88**, 083516 (2013); L. L. Vietze, P. Klos, J. Menendez, W. C. Haxton and A. Schwenk, Phys. Rev. D **91**, 043520 (2015).
 - [19] N. Anand, A. L. Fitzpatrick and W. C. Haxton, Phys. Rev. C **89**, 065501 (2014).
 - [20] J. Engle and J. Menendez, Rep. Prog. Phys. **80**, 046301 (2017); and references therein.
 - [21] D. F. Jackson-Kimball et al., Annalen der Physik, **525**, 514 (2013).
 - [22] S. K. Lamoreaux, J. P. Jacobs, B. R. Heckel, F. J. Raab, and E. N. Fortson Phys. Rev. Lett. **57**, 3125 (1986); ;Phys. Rev. Lett. **57**, 3125 (1986).
 - [23] N. J. Stone, Atomic Data and Nuclear Data Tables, **90** 75 (2005).
 - [24] J. P. Delaroche et al., Phys. Rev. C **82** 014303 (2010).
 - [25] P. Ring and P. Schuck, The Nuclear Many Body Problem (Springer, Berlin 1984).
 - [26] L. M. Robledo, R. Bernard and G. F. Bertsch, Phys. Rev. C **86**, 064313 (2012).
 - [27] J. F. Berger, M. Girod, and D. Gogny, Nucl. Phys. **A428**, 23c (1984).
 - [28] A. Bohr and B. R. Mottelson, Nuclear Structure, Volume II, (W. A. Benjamin, 1975).
 - [29] B. A. Brown and W. A. Richter, Phys. Rev. C **74**, 034315 (2006).
 - [30] W. A. Richter, S. Mkhize, and B. A. Brown, Phys. Rev. C **78**, 064302 (2008).
 - [31] B. Bally, B. Avez, M. Bender, and P.-H. Heenen, Phys. Rev. Lett. **113**, 162501 (2014)
 - [32] G. F. Bertsch and L. M. Robledo, Phys. Rev. Lett. **108**, 042505 (2012))
 - [33] H. Hergert, S. K. Bogner, T. D. Morris, A. Schwenk, K. Tsukiyama, Phys. Rep. **621**, 165 (2016).
 - [34] J. Carlson, S. Gandolfi, F. Pederiva, Steven C. Pieper, R. Schiavilla, K. E. Schmidt, and R. B. Wiringa, Rev. Mod. Phys. **87**, 1067 (2015).
 - [35] G. Hagen, T. Papenbrock, M. Hjorth-Jensen, D. J. Dean, Rep. Prog. Phys. **77**, 096302 (2014).